Preparation, *ex-situ* and *in-situ* Characterization of Gas Diffusion Media Containing and Non-Containing Carboxymethylcellulose for PEM Fuel Cells

S. Latorrata[1]*, P. Gallo Stampino[1], C. Cristiani[1], G. Dotelli[1]

[1] Politecnico di Milano, Dipartimento di Chimica, Materiali e Ingegneria Chimica ''G. Natta'', Piazza Leonardo da Vinci 32, 20133 Milano (Italy)

Received August 01, 2014; accepted March 09, 2015

1 Introduction

In recent decades Polymer Electrolyte Membrane (PEM) fuel cells have attracted scientific community attention for use as power sources in mobile and stationary applications due to low related emissions and high power densities reached [1–5]. Thus, several efforts have been spent in order to develop technologically advanced materials for improving electrical performances [6, 7]. Many studies and papers have demonstrated how water management in PEMFC, above all for the cathodic side, is one of the crucial factors affecting performances [8–12]. Gas Diffusion Medium (GDM), which is formed by a macroporous carbon cloth or carbon paper substrate (Gas Diffusion Layer, GDL) and a microporous layer (MPL), is the most relevant cell component in water management. Indeed, one of its main functions is to drain out liquid water from catalyst layer to flow channels, and as such it must be hydrophobic [9, 12–16]. Moreover, it has to be electronically and thermally conductive and to guarantee a good contact between bipolar plate and membrane electrode assembly (MEA) [16, 17]. Liquid water is generated at cathodic catalyst layer by the oxygen reduction and supplied by external humidifiers. An accumulation of this water could cause diffusion limitations and rise related mass transfer resistances due to the blocking of pores of catalyst and GDM and the consequent decrease of reactant gases supply [8, 12, 18–20]. This phenomenon can lead to water flooding, above all at high current densities values. Thus, GDM is necessary in order to guarantee the correct balance between external water from humidifiers and internal generated water [12, 14, 15, 18–20].

GDLs, with a thickness in the range of 100–400 μm, are made of carbon papers or carbon clothes, which are typically macroporous materials. Instead, MPLs are thin hydrophobic microporous layers coated onto the GDLs surface, prepared starting from aqueous dispersions of carbon black and polymer binders such as polytetrafluoroethylene (PTFE) particles.

[*] *Corresponding author, saverio.latorrata@polimi.it*

MPL layers enhance water removal and gas permeability [12, 15, 16], improve the smoothness of the GDL surface, allowing a better contact with the catalytic layer and reducing contact resistances [21]. Indeed, MPLs have been recently employed to reduce mass transport limitations, which are due to water flooding, and to improve performances, especially in the high current density region [12, 16, 22–27]. On the other hand if the electrolytic membrane was dehydrated, the performance of the fuel cell would decrease because ionic conductivity of the proton membrane is strongly dependant on water content [15, 28, 29]. Therefore, a right balance between water supply and removal is fundamental for PEMFCs performance.

Doctor blade coating technique was employed to coat GDLs [30–32]. Such a technique requires the use of non-newtonian and relatively viscous fluids. In previous papers the effect of PTFE/CB on inks stability and rheology were studied, also the final electrical performances of the cell were discussed as function of MPL formulation [30, 32]. However, during inks preparation some instability phenomena could occur due to the difficulty to disperse carbon powders in water. In the industrial practice the use of carboxymethylcellulose (CMC) is reported as viscosity and stability controller. In fact, CMC is a polysaccharide that, acting on the colloidal forces, suppresses the tendency to aggregate of solid particles thus inhibiting flocculation and preventing instability phenomena of the inks [33]. The hydrophilic nature of CMC makes its use proper to disperse powders in water-based fluids, while the shear thinning behaviour of the dispersions so obtained is suitable for doctor blade application [32, 34]. Indeed, the use of pseudoplastic shear thinning slurries is usually proposed for laboratory and industrial applications [35], when considering blade coating. Thus, in this paper, water CMC and PTFE contents were selected according to literature indications for GDLs and doctor-blade applications [13, 32]. In particular, the effect of the two different PTFE/CB ratios (12 % and 40 % w/w) was investigated. Slurries were prepared on the basis of the procedure described in [30]. The effect of CMC on rheological properties and electrical performances of single PEMFC is reported and compared with the behaviour of the CMC-free samples. Electrochemical tests, two temperature and two RHs conditions were evaluated.

2 Experimental

Commercial carbon clothes GDLs (S5, SAATI Group) were used as substrates and were previously hydrophobized by dipping in a PTFE suspension (12 % wt).

Inks were prepared according to the procedure described in previous papers [30, 32]. In order to investigate the effect of CMC addition at different PTFE contents, four inks were prepared. Two inks, PTFE12 and PTFE40, contained 12 % wt and 40 % wt of PTFE, respectively, while the other two samples, CMC-PTFE12 and CMC-PTFE40, were prepared by adding 2 % wt CMC to the above compositions. In Table 1 the relative amounts of the inks components are reported.

Table 1 Samples and amounts of the components. CB: carbon black, T: Triton X-100 (surfactant), W: water, PTFE: polytetrafluoroethylene, CMC: carboxymethylcelluse

Sample	CB/T [w/w]	CB/W [w/w]	PTFE/CB [w/w]	CMC/W [w/w]
CMC-PTFE12	5.6	0.13	0.12	0.02
CMC-PTFE40	5.8	0.13	0.40	0.02
PTFE12	5.6	0.13	0.12	–
PTFE40	5.8	0.13	0.40	–

In a typical experiment, carbon black powder, Vulcan XC72R (referred to as CB), was mixed with an appropriate amount of a 60 % wt PTFE suspension and Triton X100 as a surfactant (referred to as T) using deionised water (W) as dilutant. Such components were mixed by an UltraTurrax T25 homogenizer for 10 minutes at 8000 rpm, subsequently, CMC was added and yet mixed at the same rate; finally the PTFE suspension was added and the inks stirred for 10 minutes at 500 rpm. In case of CMC-free samples exactly the same procedure was applied except for the CMC addition step.

After preparation, the slurries were deposited onto the substrates via doctor-blade technique using a lab-scale commercial equipment K CONTROL COATER. A linear velocity of 0.042 m s^{-1} and a 40 µm gap were selected, corresponding to a shear rate of about 100 s^{-1}. The coated samples were heated in air up to 350 °C for 30 min [36].

The rheological behaviour of the inks was analysed at 20 °C with a rotational rheometer (Rheometrics DFR 200) equipped with a 40 mm parallel-plates geometry, with a gap (i.e. the width of the obtained ink) between the stationary plate and the movable one of 0.5 mm. Viscosities were investigated in the shear rates range 10^{-3}–10^{3} s^{-1}.

A Cambridge Stereoscan 360 scanning electron microscope (SEM) was used for the morphological analyses of GDMs. SEM analyses were carried out both onto the surfaces and the fracture surfaces of the samples, that were gold coated to prevent charging effects.

In order to assess the hydrophobicity of the GDMs, static contact angles of the samples were measured according to the sessile drop technique with an OCA 20 Dataphysics instrument. Values reported in this paper for each sample are the result of the average of ten measurements.

The electrochemical performances of the four GDMs were tested in a single cell assembly. The graphite bipolar plates had a single serpentine at the anode and a triple one at the cathode; the active area was 25 cm^2; the MEA was assembled using Nafion 212 membrane, whose thickness was 50 µm and the catalyst layer was coated directly onto the membrane (i.e. catalyst coated membrane, briefly CCM) with a platinum loading of 0.3 mg cm^{-2} at the anode and 0.6 mg cm^{-2} at the cathode. Hydrogen and air were used as the anodic and cathodic feedings, respectively. Flow rates were controlled and detected by a calibrated flow meter; humidity and the inlet gas temperature were controlled by external humidifiers and temperature controllers.

Experiments were carried out at two different cell temperatures (60 °C and 80 °C) under the flow rates regime of 0.20/1.00 NL min^{-1} (H_2/air); only one humidity condition was employed for the hydrogen flow (80 % RH), while two different humidity conditions (60 and 100 % RH) were adopted for the air feeding in order to evaluate the effect of low and high humidity on cathodic water management. An electronic load (RBL488-50-150-800), for measuring voltage, current and generated power, was connected to the cell. Polarization curves were recorded under galvanostatic conditions in the current density (CD) range from OCV to 0.87 A cm^{-2}, with steps of 0.085 A cm^{-2}. At each step, the resulting potential was recorded in galvanostatic mode for 420 seconds per step, at one second intervals. Potential values plotted in the steady-state polarization curves result from the averaging of the last 300 points recorded at each step in order to minimize experimental artefacts due to transient phenomena.

Electrochemical Impedance Spectra (EIS) was carried out using a Frequency Response Analyzer (FRA, Solartron 1260). All spectra were obtained over a frequency range of 0.5 Hz–1.0 kHz (10 points per decade) at the fixed current amplitude of 200 mA [37]. Impedance spectra were recorded (galvanostatic mode) at six different current densities: OCV, 0.17, 0.34, 0.52, 0.7 and 0.87 A cm^{-2}. At each current density, five spectra were collected and each value reported in the Nyquist diagram was the averaging of the five experimental points. All the experimental data were fitted using the Zview® software (Solartron).

The typical spectrum of a running fuel cell is composed by one or two arcs, representing two physical phenomena: activation polarization and mass transfer limitations. The activation polarization occurs at both electrodes, but the cathodic oxygen reduction reaction requires higher overpotential and it is slower than the anodic hydrogen oxidation. The mass transfer limitations take place when the reactants concentration decreases near the catalyst layer. This phenomenon occurs more likely when the cell works in the high current density region because higher amounts of water are produced at the cathode, increasing the risk of flooding.

The results of EIS analysis will be shown in terms of ohmic resistance trend (as a function of current density) and of overall internal resistance trend, which is the result of phenomena both of activation polarization and of mass transfer limitations.

3 Results and Discussion

In order to investigate the rheological behaviour and the time stability of the inks, the rheological measurements where performed at t = 0 h (i.e. immediately after preparation) and after 24 and 48 h of ageing.

Since Figure 1 shows that dynamic viscosities always decrease upon increasing shear rate, it can be assumed that all the samples are pseudo-plastic and shear-thinning, which makes them suitable for blade coating applications [35]. The addition of CMC increases viscosity and improves shear-thin-

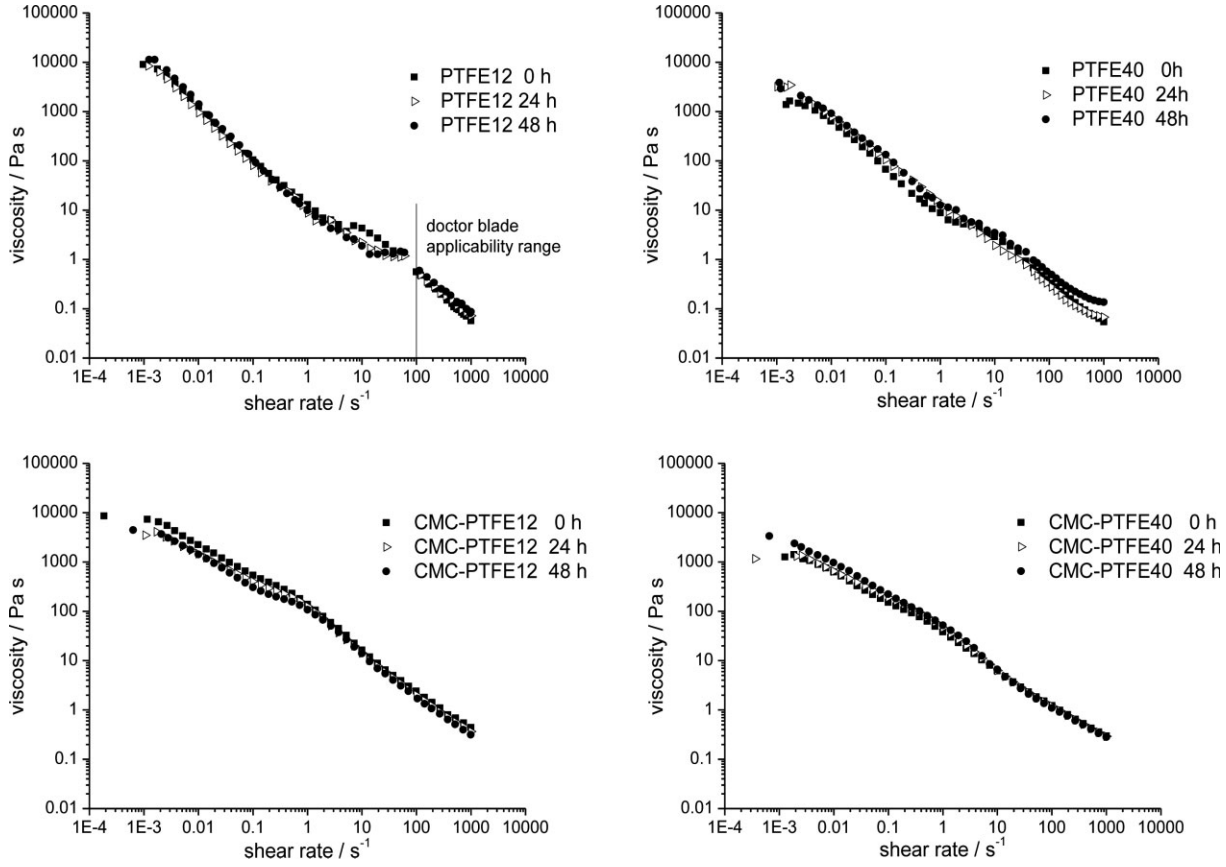

Fig. 1 Rheological curves of the inks containing and not containing CMC at different maturation times.

ning behaviour. Samples which contain a higher PTFE amount (i.e. PTFE40 and CMC-PTFE40) always have a lower viscosity with respect to the samples with 12 % wt of PTFE. In the rheological curves of CMC-free samples a marked inflection point was observed, that tentatively could be ascribed to instability of the ink due to re-aggregation of the dispersed carbon particles. In CMC-based samples such inflection point is smoother and shifted at shear rates far below than those typically applied in blade coating technique (i.e. > 100 s^{-1}) during coating deposition. Accordingly, a stabilizing effect of CMC addition is clearly evident.

No effect of the ageing time was observed: the rheological curves were always overlapped suggesting that the instability phenomena occurred in CMC-free samples are composition-dependent but not time-dependent.

SEM micrographs of the coatings surfaces upon thermal treatment are reported in Figure 2. Coatings seem to be quite homogeneous, even if they exhibit identifiable holes or cracks at the surface. Moreover, traces of the original substrate structure are somewhat evident.

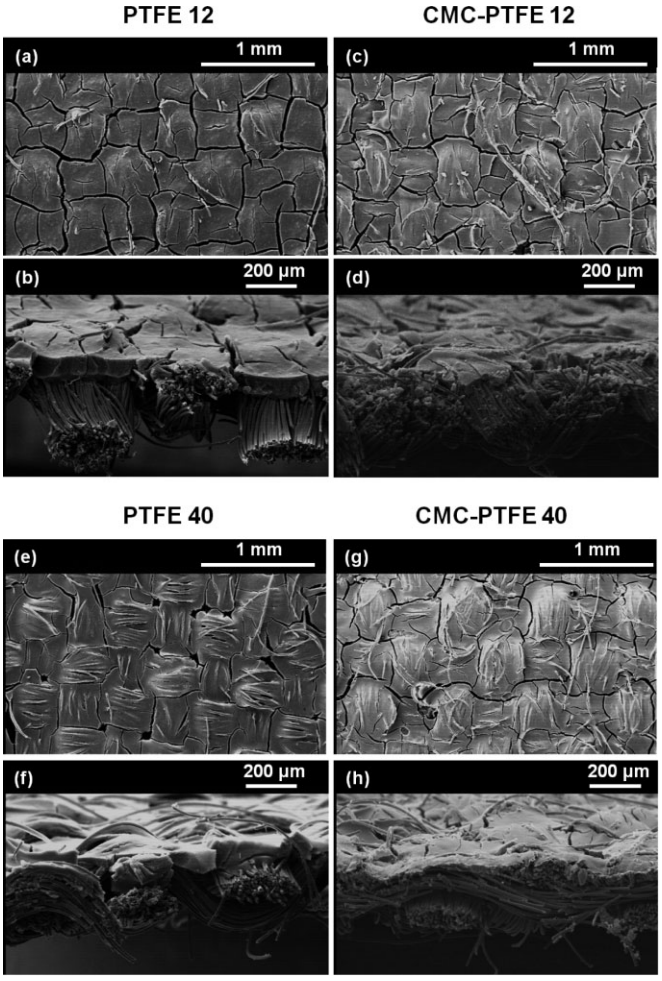

Fig. 2 SEM images of surfaces and sections of substrates coated with or without CMC-based slurries. (a), (b) PTFE12; (c), (d) CMC-PTFE12; (e), (f) PTFE40; (g), (h) CMC-PTFE40.

Since a correct measurement of the actual thickness of coatings results difficult, due to the compressible nature of substrates, only a mean range of thickness can be given: MPL thicknesses seem to be quite uniform and vary in the range 35–38 µm for samples coated with CMC-based inks and 50–70 µm for CMC-free ones. An apparent inconsistency between viscosity and layers thickness was found, because the higher viscosity, the higher coating thickness should be expected. However, the lower thickness value measured for CMC-containing coatings can be explained just with the presence of CMC itself in the ink formulation. Indeed, considering the coating theory, the relationship between viscosity and thickness is referred to the thickness of the "wet layer", i.e. before thermal treatment. Upon thermal treatment at 350 °C, CMC partially decomposes, as revealed by thermogravimetric analysis (about 40 % wt of weight loss at 350 °C, see Supplementary Material), thus this decomposition results in a final thinner layer.

The static contact angle measurements, which give indication on the hydrophobicity of the GDMs, are reported in Figure 3. Focusing on samples containing 12 % wt PTFE, a sharp difference can be noticed between the two GDMs with and without CMC. Indeed, CMC-PTFE12 exhibits an average contact angle of 129° while PTFE12 shows an average contact angle of 142°, thus more hydrophobic. On the other hand, CMC-PTFE40 and PTFE40 show practically identical contact angles. In this case, the high PTFE content of the inks levels the surfaces which become both highly hydrophobic. Moreover, the contact angle of the bare hydrophobized GDL is about 140° [36], suggesting that the presence of MPL does not lead to a significant change of hydrophobicity, except for CMC-PTFE12, whose reduced measured hydrophobicity can be ascribed to residues of decomposition of CMC (hydrophilic) which cannot be hindered by PTFE content because too low.

The steady-state current density-potential curves and current density-power density curves of the PEMFC assembled with the four different types of GDM are all reported in Figure 4 and Figure 5.

By comparing the polarization curves of samples CMC-PTFE12 and PTFE12, a significant improvement in the electrical performance of the sample with the CMC-PTFE12 occurs when the cell operates at low humidity (RH 80-60) and high temperature (T80) on the entire range of current density (CD) investigated (Figure 4C). Instead, at both low temperature and low relative humidity the best performances of the CMC-PTFE12 sample are confined to the region of middle-low current densities (i.e. < 0.6 A cm^{-2}, Figure 4A). On the contrary, at high humidity (RH 80-100), the presence of CMC in the MPL seems to be detrimental, causing an inefficient water management which results in poor electrical performances and sudden voltage drop (Figure 4B and Figure 4D).

From Figure 5, it is easy to identify such a behaviour even when the PTFE amount is higher (i.e. CMC-PTFE40 and PTFE40 samples). However, at low humidity (Figure 5A and Figure 5C) the performance of the CMC-PTFE40 sample is better than the CMC-PTFE12 one, even at 60 °C, because of the

higher PTFE amount which leads to a better hydrophobic degree. Electrical performance of the CMC-containing sample (i.e. CMC-PTFE40) is penalized when cell works at high current densities under conditions of high relative humidity, pointing out again a poor water management in these particular operating conditions (Figure 5B and Figure 5D).

Therefore, it can be stated that the presence of CMC in MPLs led to better electrical performances with respect to standard composition based MPLs at low relative humidity: for CMC-PTFE40 this is true for both experimented temperatures, while CMC-PTFE12 exhibited a better performance than PTFE12 only at 80 °C. CMC acts as a sort of water reservoir: at low humidity it prevents membrane dehydration. Drawbacks arise at high humidity because CMC absorbs too much water and this likely limits the rate of reactions and penalizes the electrical performances.

Examples of typical impedance spectra of the running fuel cells, assembled with the different GDMs, at three different current densities (low, medium and high) and operating conditions of 80 °C and RH 80 %–60 % (A–C) are shown in Figure 6.

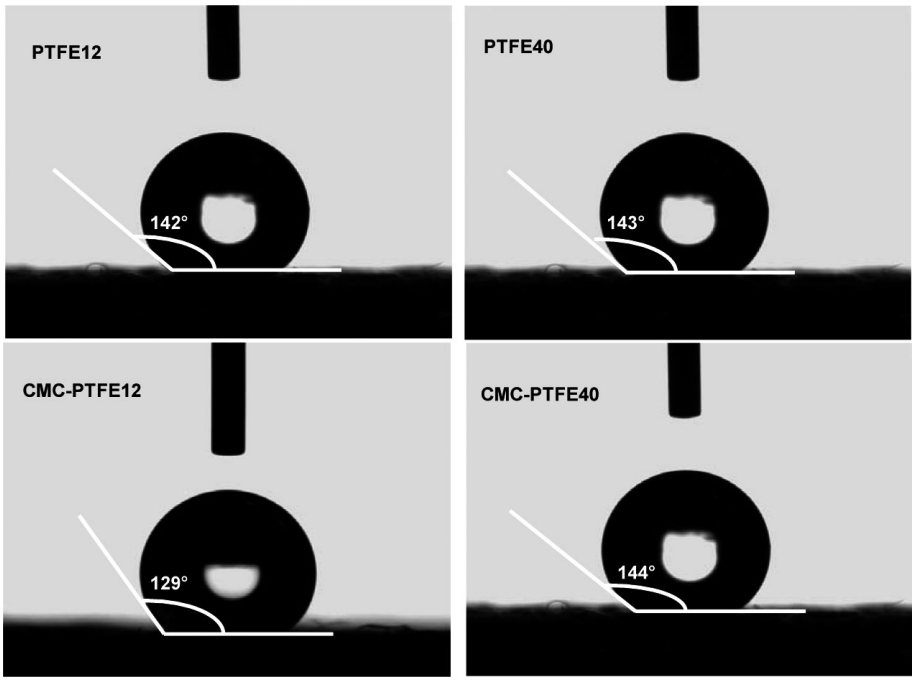

Fig. 3 Results of the contact angle analysis on the four investigated surfaces.

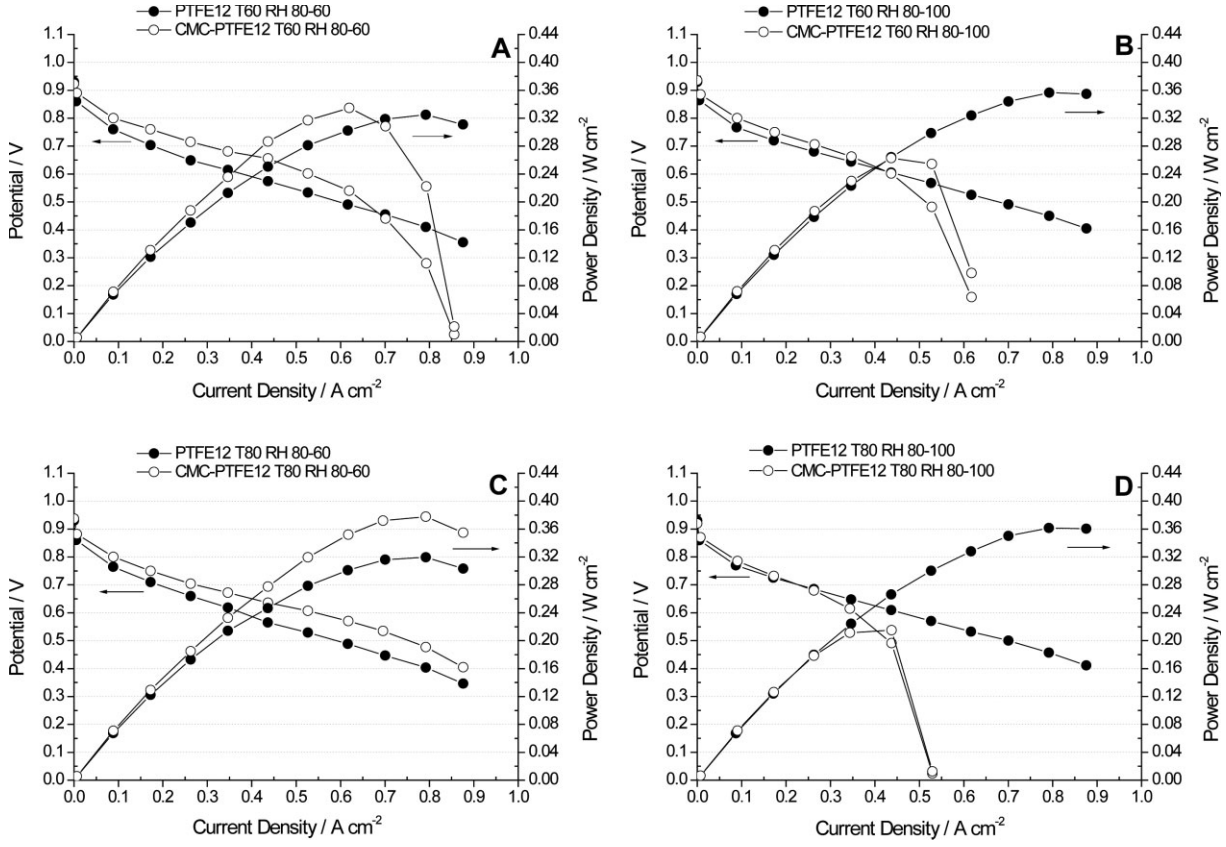

Fig. 4 Polarization curves of samples CMC-PTFE12 and PTFE12; (A) T60 RH 80-60; (B) T60 RH 80-100; (C) T80 RH 80-60; (D) T80 RH 80-100.

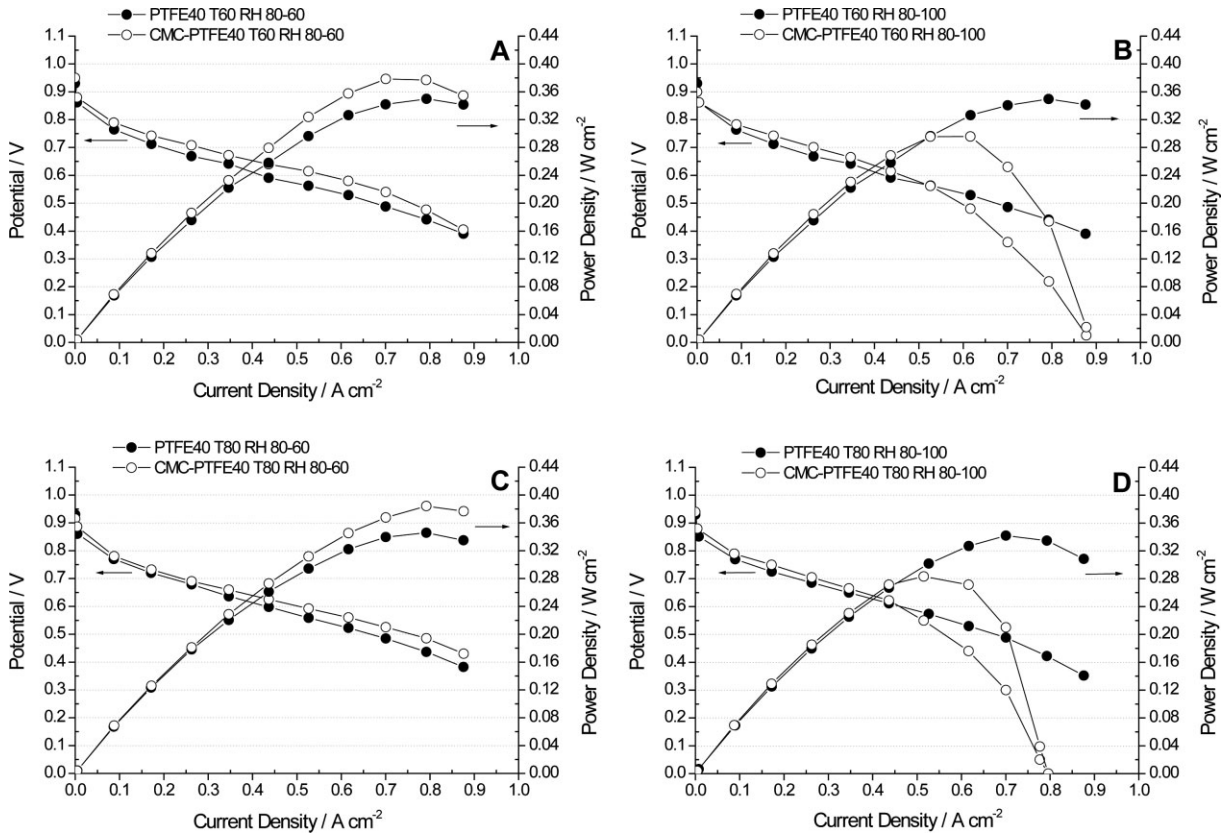

Fig. 5 Polarization curves of samples CMC-PTFE40 and PTFE40; (A) T60 RH 80-60; (B) T60 RH 80-100; (C) T80 RH 80-60; (D) T80 RH 80-100.

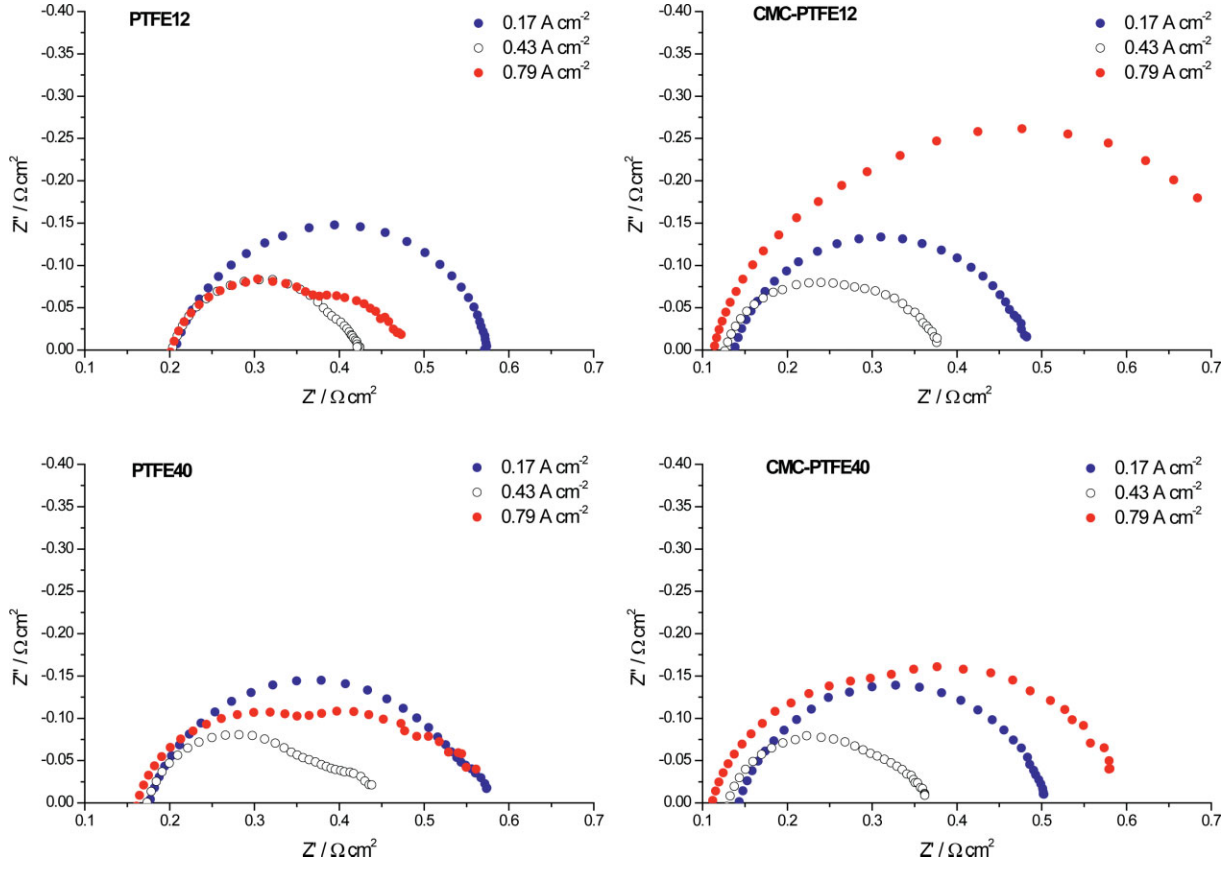

Fig. 6 Impedance spectra obtained at low, medium and high CD and operating conditions of 80 °C and RH 80 %–60 % (A–C).

It is evident that, for no-CMC containing samples, ohmic resistance (i.e. the intercept of the spectrum with the real axis at high frequency) does not change substantially with the increase of current density, while it decreases somewhat when CMC is present. The values exhibited by non-containing CMC MPLs are higher than those of CMC-based MPLs, suggesting a positive effect of CMC in reducing ohmic resistance in each condition.

Generally, at low current density (i.e. 0.17 A cm^{-2}) the impedance spectra of all samples showed only one arc; this phenomenon may be ascribed to the activation polarization process [38, 39].

In the medium current density region (i.e. 0.43 A cm^{-2}), two arcs are distinguishable: the higher frequency one is attributable to the polarization process due to charge transfer limitations, while the lower frequency one points out the presence of some mass transfer limitations [38]. For CMC-containing MPLs the diffusion contribution is more pronounced, above all at high current density (i.e. 0.79 A cm^{-2}), when it can also obscures the activation-polarization one.

A comparison of the ohmic resistances, Rs, of the four GDMs is reported in Figure 7, for all the experimental conditions of temperature and RH. CMC-containing GDMs are able to reduce ohmic resistance due to the presence of CMC which retains water and drives to a better hydration of the membrane. When cathodic RH is 100 %, CMC-PTFE12 sample exhibits a slightly higher ohmic resistance than CMC-PTFE40 sample at both temperatures and for each current density value, whereas at cathodic RH of 60 % it shows the lowest values of Rs. At low humidity the degree of the membrane hydration is definitely crucial and consequently, in CMC-PTFE40 sample, due to the higher dielectric content (i.e. more PTFE), Rs is higher. Moreover, it decreases as a function of current density. This result can be ascribed to the membrane proton conductivity which increases with the degree of humidification: at low humidity, Rs decreases due to a larger water amount produced upon increasing current density. On the contrary, when cathodic RH is maximum, membrane is totally saturated and, apart from composition, even MPL thickness can likely play a role in determining ohmic resistance: indeed, CMC-PTFE40, with a lower thickness (see Figure 2), also exhibits a lower Rs. The lack of some data when current density becomes high is due to voltage drop showed in Figure 4 and Figure 5.

At each operating condition, MPLs without CMC show higher ohmic resistances. This result again underlines the improvement introduced by CMC in hydrating membrane and thus in reducing ohmic resistance. Generally Rs does not change significantly with the increase of current density for each condition.

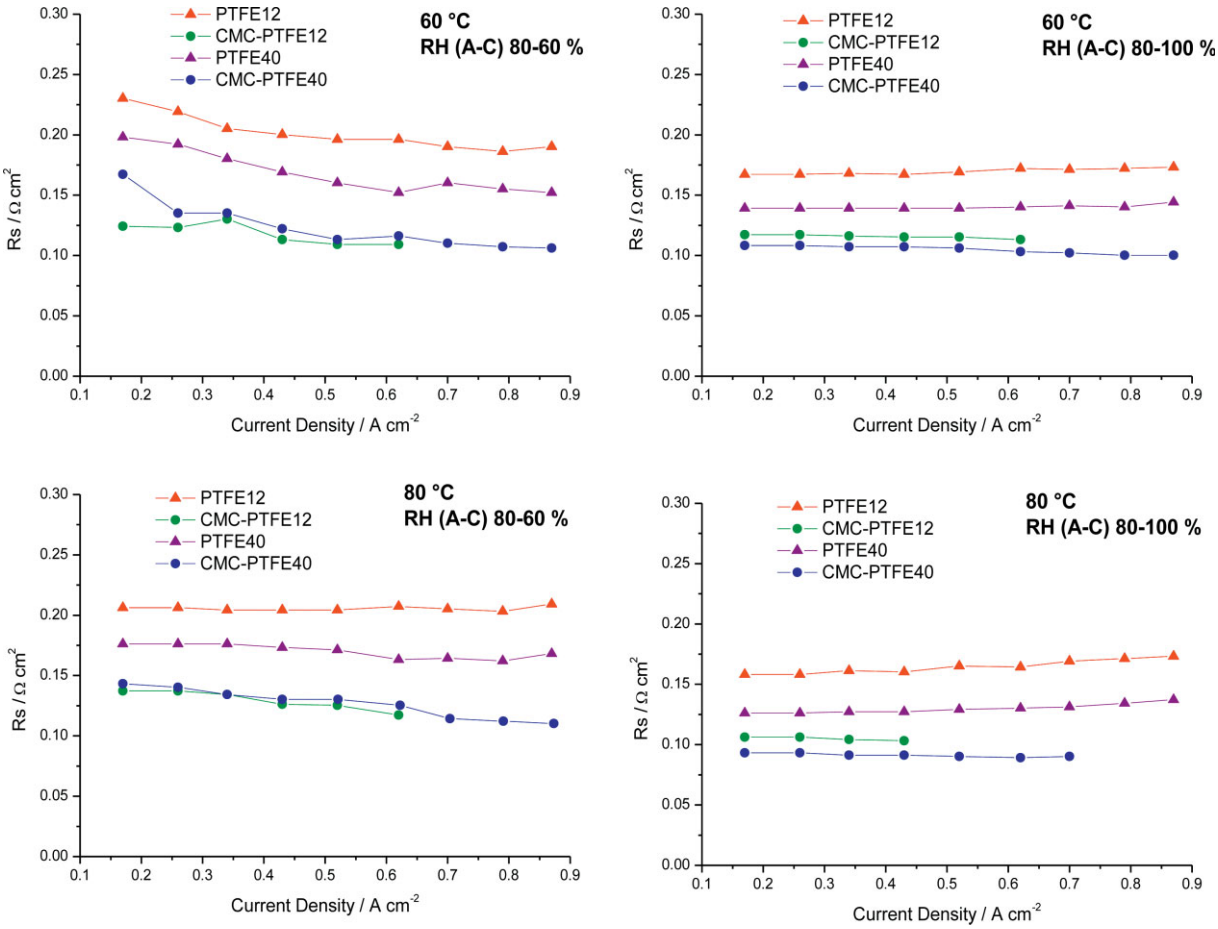

Fig. 7 Trend of Rs parameters as a function of CD for the four samples at each operating condition.

A comparison of the overall internal resistance, i.e. the sum of charge transfer resistance (or polarization resistance, Rp) and of mass transfer one (or diffusion resistance, Rd), for the four samples is reported in Figure 8.

When cathodic RH is 60 %, Rp+Rd increases upon increasing current density from 0.5 - 0.6 A cm^{-2}. At high humidity this behaviour is more evident, due to more pronounced mass transfer limitations. Indeed, the polarization resistance keeps constant or decreases somewhat at high current densities and this is usually ascribed to the lowering of the anode charge transfer resistance [38, 40]; thus the increase of the sum Rp+Rd can be ascribed to diffusion resistance, which is more dramatic for CMC-containing MPLs due to hydrophilic feature of CMC. These trends can also explain the voltage drop observed in Figure 4 and Figure 5 at high cathodic RH, above all for CMC-PTFE12. Even CMC-PTFE40 shows similar total resistances, but it succeeded in reaching elevated current density values due to the high content of hydrophobic agent, PTFE. No-containing CMC samples show a more restrained Rp+Rd increase at each operating condition, due to the absence of CMC which retains water at high current densities.

Finally, when CMC is present, an increase of temperature, if RH is fixed, leads to a better situation (i.e. a lower Rp+Rd) because of a faster evaporation of water. However, if compared to samples with the same PTFE content, it is clear that CMC presence causes a worsening of water management in the region of medium and high current densities, due to its hydrophilicity.

4 Conclusions

The adopted preparation route allowed to obtain inks with a shear thinning behaviour in the whole investigated shear rate range, thus suitable for MPL deposition via the doctor blade technique. In particular, the addition of CMC has a positive effect on stability and shear thinning behaviour of the prepared inks. MPLs deposited on carbon cloth substrates are quite homogeneous, even if some cracks are evident because of thermal treatment. All the samples are hydrophobic but the presence of residual CMC limits this feature.

The electrochemical performance of the fuel cell assembled with the GDLs coated with the four prepared inks showed that the CMC-PTFE40 drives to an increase of the maximum value of power density at low relative humidity and at both temperature values investigated; instead, CMC-PTFE12 leads to a better electrochemical performance only at high temperature and low relative humidity.

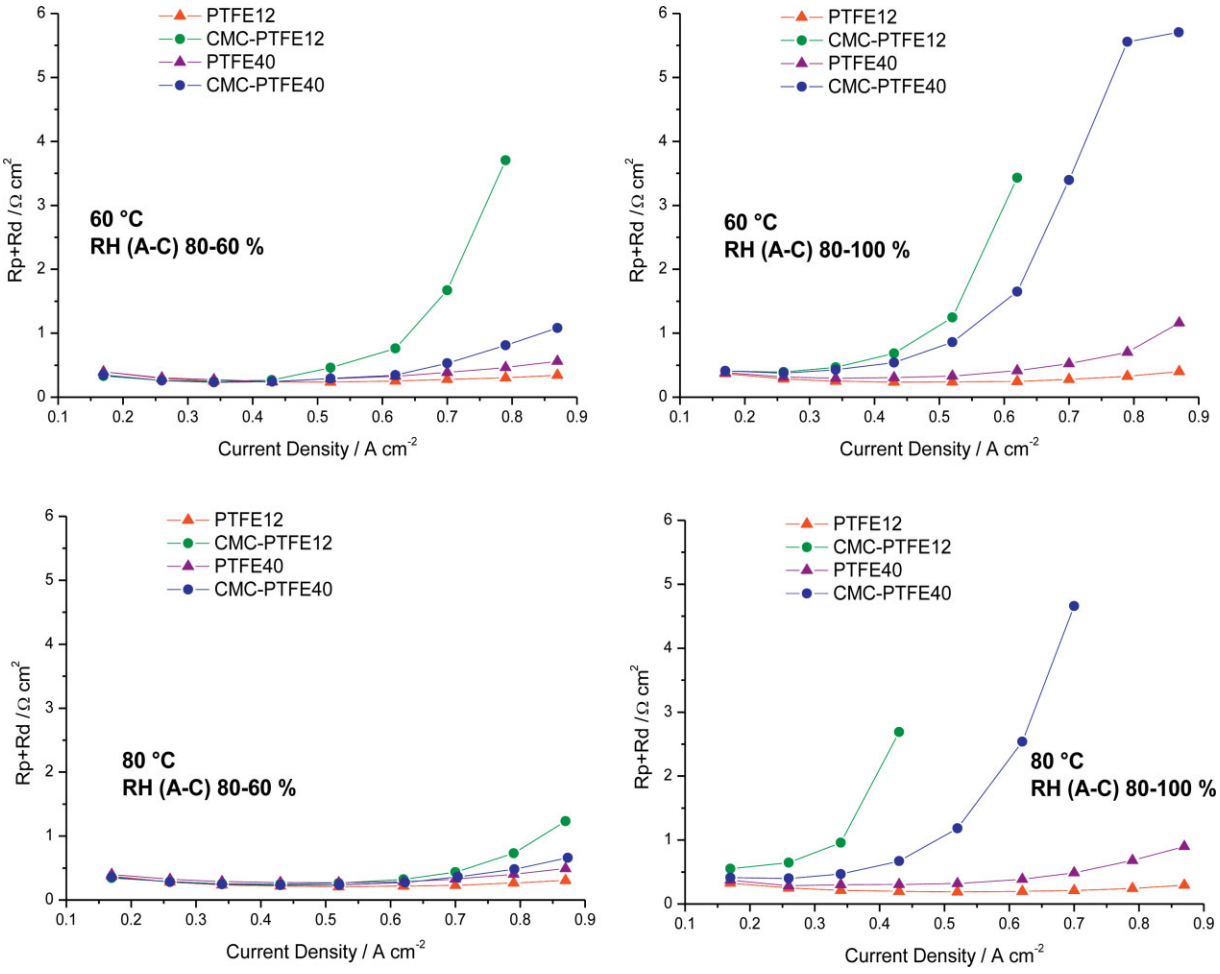

Fig. 8 Trend of the sum of Rp and Rd parameters as a function of CD for the four samples at each operating condition.

References

[1] A. Bauen, D. Hart, *J. Power Sources* **2000**, *86*, 482.
[2] M. M. Hussain, I. Dincer, X. Li, *Appl. Therm. Eng.* **2007**, *27*, 2294.
[3] L. Venturelli, P. E. Santangelo, P. Tartarini, *Appl. Therm. Eng.* **2009**, *29*, 3469.
[4] O. Erdinc, M. Uzunoglu, *Renew. Sustain. Energy Rew.* **2010**, *14*, 2874.
[5] Y. Wang, K. S. Chen, J. Mishler, S. C. Cho, X. C. Adroher, *Appl. Energy* **2011**, *88*, 981.
[6] A. C. Dupuis, *Prog. Mater. Sci.* **2011**, 56, 289.
[7] S. Subianto, M. Pica, M. Casciola, P. Cojocaru, L. Merlo, G. Hards, D. J. Jones, *J. Power Sources* **2013**, *233*, 216.
[8] U. H. Jung, S. U. Jeong, K. T. Park, H. M. Lee, K. Chun, D. W. Choi, S. H. Kim, *Int. J. Hydrogen Energy* **2007**, *32*, 4459.
[9] J. Chen, T. Matsuura, M. Hori, *J. Power Sources* **2004**, *131*, 155.
[10] G. G. Park, Y. J. Sohn, T. H. Yang, Y. G. Yoon, W. Y. Lee, C. S. Kim, *J. Power Sources* **2004**, *131*, 182.
[11] D. H. Ahmed, H. J. Sung, J. Bae, D. R. Lee, *Int. J. Heat Mass Tran.* **2008**, *51*, 2006.
[12] G. Unsworth, N. Zamel, X. G. Li, *Int. J. Hydrogen Energy* **2012**, *37*, 5161.
[13] S. Park, J. W. Lee, B. N. Popov, *J. Power Sources* **2008**, *177*, 457.
[14] T. Kitahara, T. Konomi, H. Nakajima, *J. Power Sources* **2010**, *195*, 2202.
[15] T. Kitahara, H. Nakajima, M. Inamoto, K. Shinto, *J. Power Sources* **2014**, *248*, 1256.
[16] S. Park, J. W. Lee, B. N. Popov, *Int. J. Hydrogen Energy* **2012**, *37*, 5850.
[17] L. Cindrella, A. M. Kannan, J. F. Lin, K. Saminathan, Y. Ho, C. W. Lin, J. Wertz, *J. Power Sources* **2009**, *194*, 146.
[18] T. Kim, S. Lee, H. Park, *Int. J. Hydrogen Energy* **2010**, *35*, 8631.
[19] F. Cao, G. X. Pan, P. S. Tang, H. F. Chen, *J. Power Sources* **2012**, *216*, 395.
[20] Y. T. Cheng, H. L. Tang, M. Pan, *J. Power Sources* **2012**, *198*, 190.
[21] M. B. Ji, Z. D. Wei, *Energies* **2009**, *2*, 1057.
[22] C. S. Kong, D. Y. Kim, H. K. Lee, Y. G. Shul, T. H. Lee, *J. Power Sources* **2002**, *108*, 185.
[23] C. J. Tseng, S. K. Lo, *Energy Convers. Manage* **2010**, *51*, 677.
[24] H. K. Atiyeh, K. Karan, B. Peppley, A. Phoenix, E. Halliop, J. Pharoah, *J. Power Sources* **2007**, *170*, 111.
[25] H. L. Tang, S. L. Wang, M. Pan, R. Z. Yuan, *J. Power Sources* **2007**, *166*, 41.
[26] T. Kitahara, H. Nakajima, K. Mori, *J. Power Sources* **2012**, *199*, 29.
[27] T. L. Liu, C. Pan, *J. Power Sources* **2012**, *207*, 60.
[28] D. Hyun, J. Kim, *J. Power Sources* **2004**, *126*, 98.
[29] S. J. Peighambardoust, S. Rowshanzamir, M. Amjadi, *Int. J. Hydrogen Energy* **2010**, *35*, 9349.
[30] E. S. Lee, K. H. Yang, H. R. Jung, T. H. Kim, S. K. Han, J. K. Lee, Y. H. Seo, J. H. Park, *US Patent 2009/0011308 A1*, **2009**.
[31] A. Arthur Tracton, *Coatings Materials and Surface Coatings*, Taylor and Francis, Boca Raton, Florida, **2007**.
[32] S. Latorrata, P. G. Stampino, E. Amici, R. Pelosato, C. Cristiani, G. Dotelli, *Solid State Ionics* **2012**, *216*, 73.
[33] K. Benyounes, A. Mellak, A. Benchabane, *Energy Source Part A* **2010**, *32*, 1634.
[34] T. M. Sullivan, S. Middleman, *J. Non-Newton. Fluid* **1986**, *21*, 13.
[35] A. Arthur Tracton, *Coatings Technology Handbook*, Taylor & Francis, Boca Raton, Florida, **2005**.
[36] P. G. Stampino, C. Cristiani, G. Dotelli, L. Omati, L. Zampori, R. Pelosato, M. Guilizzoni, *Catal. Today* **2009**, *147*, S30.
[37] N. Wagner, E. Gulzow, *J. Power Sources* **2004**, *127*, 341.
[38] N. Wagner, *J. Appl. Electrochem.* **2002**, *32*, 859.
[39] S. Asghari, A. Mokmeli, M. Samavati, *Int. J. Hydrogen Energy* **2010**, *35*, 9283.
[40] P. Gallo Stampino, L. Omati, C. Cristiani, G. Dotelli, *Fuel Cells* **2010**, *10*, 270.